

Shape Deformation and Phase Separation Dynamics of Two-Component Vesicles

Takashi Taniguchi*

Department of Physics, Kyoto University, Kyoto 606, Japan

(Received 23 October 1995)

We numerically study dynamics of shape deformations of vesicles resulting from intramembrane phase separation. At off-critical compositions resultant vesicle shapes closely resemble the echinocytosis of red blood cells, while at the critical composition a bicontinuous domain structure emerges. The coarsening process of domain structures on such a deformable surface is considerably slower than that on a rigid surface. The total length of domain boundaries N_{DB} decreases as $t^{-1/3}$ for the rigid sphere, whereas in the present system $N_{DB} \approx t^{-z}$ ($z \approx 0.1$) at the late stage due to the coupling between the shape and the phase separation. [S0031-9007(96)00353-5]

PACS numbers: 87.22.Bt, 64.60.Cn, 68.15.+e

Since a seminal bending elastic model of the equilibrium shape of fluid membranes by Helfrich [1], a wide variety of shape transformations of closed fluid membranes, like red blood cells, has been studied extensively from both experimental and theoretical points of view [2]. This model simply treats membranes as a laterally homogeneous elastic layer without internal degrees of freedom. Nevertheless, it has succeeded in explaining equilibrium shapes of the erythrocyte.

It has recently been recognized, however, that internal degrees of freedom of membranes can crucially influence their shapes. An example is the transition from a biconcave shape of erythrocytes to a *crenated* one (*echinocytosis*) [3–5]. Such a transition cannot be explained by the original bending elastic model and the origin of such a transition is *not yet clear*. It has been pointed out that a local asymmetry in the composition between the two halves of the bilayer plays an important role in the formation of the crenated shape [4,5]. Another example is given by shape deformations induced by a phase separation of amphiphiles constituting the membrane [5–13]. It has been observed that a phase separation occurs on a two-component artificial membrane, where phase separated domains prefer increase or decrease of local curvatures depending on the local composition of the membrane [13]. In addition, it has been reported that in a two-component system the line tension of domain boundaries can cause a budding [12]. Here, in order to study the shape deformation accompanied by a lateral phase separation, we consider a two-component vesicle as the simplest model of real biomembranes composed of several kinds of amphiphiles. Up to now, the studies on two-component vesicles have been limited to those of axisymmetric equilibrium states [9–12] and dynamics of fluid membranes has not yet been fully studied for two-component membranes [14,15] and even for single-component ones [16,17].

In this Letter, using a purely dissipative dynamical model of a two-component vesicle, we simulate dynamics of the shape deformation and in-plane phase separation,

where an axisymmetric profile of vesicles is *not* assumed. The vesicle is represented by a two dimensional (2D) closed surface S parametrized by $\{u\} \equiv \{u^1, u^2\}$. For simplicity, we assume that one of the inner or the outer layers of the bilayer is composed of two kinds of amphiphiles, while the other is composed of a single component [18]. The order parameter ϕ is defined as the local difference between the concentration of A amphiphile ϕ_A and that of B amphiphile ϕ_B per unit area in the two-component area, i.e., $\phi = \phi_A - \phi_B$. In terms of ϕ , the two-component vesicle has the free energy functional $F = F_1 + F_2 + F_3$,

$$F_1 = \frac{\kappa}{2} \int (H - H_{sp})^2 \sqrt{g} d^2u + PV, \quad (1)$$

$$F_2 = \int \left\{ \frac{1}{2} \xi^2 g^{\alpha\beta} \phi_{,\alpha} \phi_{,\beta} + f(\phi) \right\} \sqrt{g} d^2u, \quad (2)$$

$$F_3 = \Lambda \int \phi H \sqrt{g} d^2u. \quad (3)$$

F_1 is the bending elastic energy where κ is the bending elasticity modulus, $H/2$ the mean curvature, H_{sp} the *homogeneous* spontaneous curvature, $\sqrt{g} d^2u$ the area element, P the pressure difference across the vesicle, and V the enclosed volume. F_2 is the Ginzburg-Landau free energy where ξ is a correlation length, $g^{\alpha\beta}$ the contravariant metric tensor, and $X_{,\alpha} \equiv \partial X(u)/\partial u^\alpha$ for any X . F_3 provides the coupling energy between the shape and the phase separation, Λ being a coupling constant. The resultant *local* spontaneous curvature arises from local asymmetry in the composition between two halves of the bilayer [5–11]. In order to get a simple description of dynamics, it is convenient to use a *body coordinate system*, in which *the coordinate* $\{u\}$ assigned to a material point is invariant throughout shape deformations. Then, the position vector of a material point $\{u\}$ at a time t is expressed as $\mathbf{r} = \mathbf{r}(u, t)$.

So far, equilibrium states of two-component vesicles have been studied by minimizing the total free energy F

under two constraints: (i) a fixed total area of the vesicle and (ii) a conserved total difference of the number of the amphiphiles A and B in each of the two sides of the bilayer [7–12,19]. In our dynamical model we reconsider these two constraints as follows. The membrane is highly incompressible due to a hydrophobic property of the tail of amphiphiles and a repulsive short-ranged interaction among the amphiphiles. If we consider dynamics on longer time scales than the characteristic relaxation time of the fluctuations of the local membrane area, fluid membranes can be assumed to be (i') *locally incompressible*. Using the body coordinate system, a mathematical expression of this constraint can be written as $\delta\sqrt{g} = 0$ which is the variation of an areal element due to the deformation $\mathbf{r}(u) \mapsto \mathbf{r}(u) + \delta\mathbf{r}(u)$. The simplest dissipative model reads

$$\frac{\partial \mathbf{r}(u, t)}{\partial t} = -L_r \frac{\delta}{\delta \mathbf{r}(u, t)} \left[F + \int \gamma(u, t) \sqrt{g} d^2u \right], \quad (4)$$

where L_r is a kinetic coefficient. The incompressibility condition for the local area of the vesicle (i') is guaranteed by a local Lagrange multiplier $\gamma(u)$ [20]. In the present model, hydrodynamic effects are entirely neglected. Our model will be justified when the vesicle is immersed in a highly viscous fluid where hydrodynamic flows are immediately overdamped [16]. Using Eqs. (1)–(4), the equation of motion can be explicitly expressed as $\partial \mathbf{r}(u, t)/\partial t = -L_r[A_\perp \mathbf{n} + A^\alpha \mathbf{g}_\alpha]$, where \mathbf{g}_α and \mathbf{n} are the tangential vector and the normal unit vector to S , respectively [21]. A_\perp and A^α are expressed as

$$\begin{aligned} A_\perp &= \frac{\kappa}{2} [(H - \bar{H}_{\text{sp}})(-H^2 - H\bar{H}_{\text{sp}} + 4K) - 2H|\alpha] \\ &\quad + P - \xi^2 \phi_{,\alpha} \phi_{,\beta} b^{\alpha\beta} \\ &\quad + \Lambda [2K(\phi - \langle \phi \rangle) - \phi|_\alpha] + \bar{\gamma} H, \\ A^\alpha &= \xi^2 (\phi_{,\alpha} \phi_{,\beta})|_\beta - \Lambda H \phi_{,\alpha} - \bar{\gamma}^\alpha \end{aligned} \quad (5)$$

where $\langle \phi \rangle$ is the surface average of ϕ , $\bar{H}_{\text{sp}} \equiv H_{\text{sp}} - \frac{\Lambda}{\kappa} \langle \phi \rangle$, $\bar{\gamma} \equiv \gamma + [\xi^2 (\nabla \phi)^2 / 2 + f(\phi)] + \kappa (H_{\text{sp}}^2 - \bar{H}_{\text{sp}}^2) / 2$, $b_{\alpha\beta}$ is a curvature tensor, $H = \text{Tr}(b_\alpha^\beta)$, $K = \det(b_\alpha^\beta)$ the Gaussian curvature, $X^\beta|_\alpha \equiv X_{,\alpha}^\beta + \Gamma_{\alpha\gamma}^\beta X^\gamma$ the covariant derivative where $\Gamma_{\alpha\beta}^\gamma$ denotes the Christoffel symbol, and the notation $X|_{\alpha\beta}$ is the abbreviation of $X|_\alpha|_\beta$. The operator $|_\alpha$ is equivalent to the Laplace-Beltrami operator Δ_{LB} which is used as the Laplacian in a curved space [2]. Obviously the equilibrium conditions are given by $A_\perp = A^\alpha = 0$, and the equation of equilibrium shape for a laterally homogeneous vesicle is given by $A_\perp = A^\alpha = 0$ and $\phi = \langle \phi \rangle$ [22]. The last three terms of A_\perp are related to the local shape deformations caused by the spatial variation of ϕ . The third term represents the effect of the line tension of domain boundaries [12]. The fourth term yields deformations coming from the local asymmetry in the composition between the inner and outer layers [4,5,13]. In the last term, $\bar{\gamma}(u)$ plays the role of an effective local surface tension. The tangential force A^α yields lateral motion keeping the local area constant.

Second, we also reconsider the constraint (ii). The change of ϕ on a surface element per unit time is given by the difference between the amount of amphiphiles diffusing into the element and that diffusing out of it. Thus (ii') the *equation of lateral continuity* $\partial \phi / \partial t + j^\alpha|_\alpha = 0$ will be assumed instead of the static constraint (ii). The diffusion flux j^α of the order parameter is driven by the lateral gradient of the local chemical potential $\mu(u) \equiv \delta F / \delta \phi(u)$, i.e., $j_\alpha = -L_\phi \mu_{,\alpha} = -L_\phi [\delta F / \delta \phi]_{,\alpha}$ where L_ϕ is a kinetic coefficient. The dynamic equation of ϕ is thus [23]

$$\frac{\partial \phi(u, t)}{\partial t} = L_\phi [-\xi^2 \phi|_\beta^\beta + f'(\phi) + \Lambda H]|_\alpha. \quad (6)$$

The equation for $\bar{\gamma}$ follows from the incompressibility condition $\partial \sqrt{g} / \partial t = \mathbf{g}^\alpha \cdot (\mathbf{r} / \partial t)_{,\alpha} \sqrt{g} = 0$ [16] as

$$\begin{aligned} \bar{\gamma}|_\alpha - H^2 \bar{\gamma} + \xi^2 [b^{\alpha\beta} H \phi_{,\alpha} \phi_{,\beta} - (\phi_{,\alpha} \phi_{,\beta})|_{\alpha\beta}] + \frac{\kappa}{2} [H(H - \bar{H}_{\text{sp}})(H^2 + H\bar{H}_{\text{sp}} - 4K) + 2HH|_\alpha \\ + \Lambda [H \phi|_\alpha + (H \phi_{,\alpha})|_\alpha - 2KH(\phi - \langle \phi \rangle)] - PH = 0. \end{aligned} \quad (7)$$

We have numerically solved the coupled equations (4)–(7) to study ordering dynamics of a two-component vesicle quenched from an initial disordered state of ϕ at a high temperature to a coexistent state of ϕ at a low temperature [21]. In the initial state, the vesicle is spherical. The vesicle surface is discretized using a deformable triangular lattice with N -lattice points ($N = 9002$). Numerical errors violating the fixed local area constraint have been suppressed below a harmless level by using a penalty functional for local areas [24]. In all simulations performed here, we have set $L_r = 0.25$, $L_\phi = \xi = 1$, $\kappa = 2$, $H_{\text{sp}} = P = 0$. The initial radius of the vesicle is $r_0 = 22.27$ and the potential is $f =$

$-\phi^2/2 + \phi^4/4$. Integration was performed using the Euler scheme, in which $\Delta t = 0.01$ is used for $t \leq 100$, and $\Delta t = 0.01$ or $\Delta t = 0.005$ is used for $t \geq 100$ depending on the magnitude of the shape deformation and the coupling constant Λ . In Fig. 1 typical shape deformations of a two-component vesicle at $t = 300$ and $\Lambda = 0.5$ are shown with (I) an initial state. The surface average $\langle \phi \rangle$ vanishes in (a) (a critical quench) and is (b) $\langle \phi \rangle = 0.3$ and (c) $\langle \phi \rangle = -0.3$ (off-critical quenches). The vesicle shape in (b) closely resembles the echinocytosis of erythrocytes, and that in (c) seems to correspond to the invagination. The bicontinuous structure in Fig. 1(a) is still transient. It might eventually

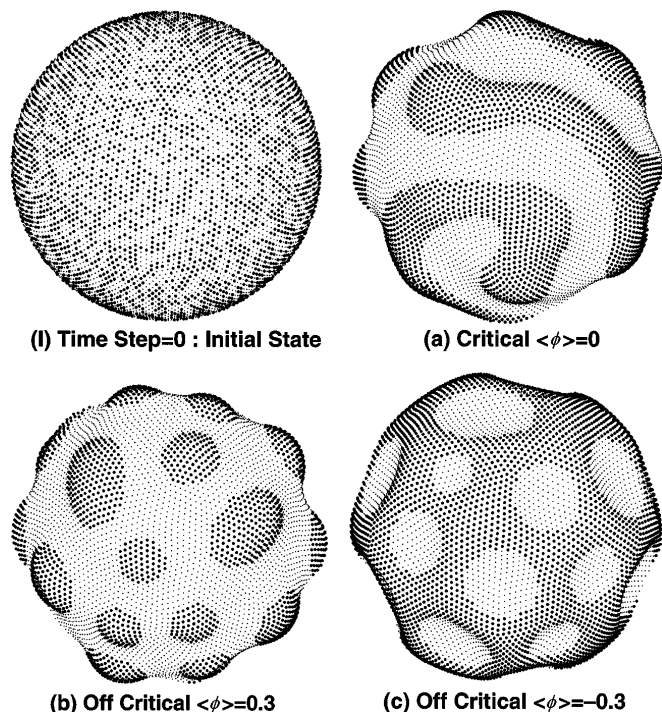


FIG. 1. Orthogonal projections of vesicle shapes: (I) the initial state, (a) a critical quench $\langle\phi\rangle = 0$, and off-critical quenches (b) $\langle\phi\rangle = 0.3$ and (c) $\langle\phi\rangle = -0.3$ at $t = 300$. The filled circles represent the sites where $\phi < \langle\phi\rangle$. There is no exaggeration of the vesicle shape along the radial direction.

change into a budded state with only two domains of ϕ , because such a budded state can be the free energy minimum for axisymmetric two-component vesicles at the critical composition [11,12]. Throughout all the simulations, the deviation of the total area $S(t)$ from the initial value $S(0)$ is within $\pm 0.26\%$ of $S(0)$ and the deviation of the local area $\sigma = \{\sum_{i=1}^N [dS(t, i)/dS(0, i) - 1]^2/N\}^{1/2}$ is within 1.08%, where $dS(t, i)$ is the local area assigned to the i th lattice point. The number of lattice points located at domain boundaries N_{DB} [25] which is proportional to the total length of domain boundaries, is shown as functions of t for critical quench in Fig. 2, and for off-critical quench in Fig. 3. Here (1) $\Lambda = 0.8$, (2) $\Lambda = 0.5$, and (3) $L_r = 0$ and $\Lambda = 0$ in the two figures. Case (3) corresponds to phase separation on a rigid sphere. As can be seen from Figs. 2 and 3, the deformations and coarsening for all cases (a)–(c) become slower with increasing Λ [26]. The total length of domain boundaries is confirmed to decrease as $t^{-1/3}$ for the rigid sphere case (3) in Figs. 2 and 3 [27] and as in the usual case of a conserved system on a 2D flat surface. In the present system the coarsening becomes significantly slowed down in the presence of the coupling. The effective exponent of $N_{DB} \approx t^{-z}$ for $\Lambda = 0.8$ at $t = 300$ is approximately $z \approx 0.1$.

This slowing down of the coarsening arises from the local coupling of ϕ to the deformation of the membrane.

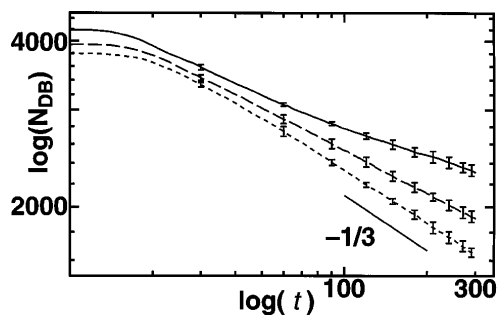


FIG. 2. Log-log plots of N_{DB} versus time for three critical quenches $\langle\phi\rangle = 0$, (1) $\Lambda = 0.8$ (solid line), (2) $\Lambda = 0.5$ (dashed line), and (3) $L_r = 0$ and $\Lambda = 0$ (dotted line). The last case (3) is the spinodal decomposition on a rigid perfect sphere. The guide line is $N_{DB} \sim t^{-1/3}$. The curves of N_{DB} for different Λ 's are averages over five independent runs.

The sum $F_1 + F_3$ is lowered when phase separated domains have local curvature $\Lambda\phi/\kappa$. This coupling thus stabilizes the domain structure against further coarsening with smaller curvatures and competes with the driving force of coarsening due to the boundary energy from F_2 . It is not clear at present whether the coarsening stops at an intermediate stage or the system ultimately reaches a budded state.

In conclusion, we simulated the shape deformation and phase separation dynamics on two-component 3D vesicles after critical and off-critical quenches using a purely dissipative model with the two local constraints: (i') the local incompressibility of membrane area and (ii') the lateral diffusion of the order parameter. The local coupling of the curvature and the composition of the membrane [4–11] and the line tension at domain boundaries arising from $\xi^2(\nabla\phi)^2$ in F_2 [12] strongly influence the formation of protrusions on the membrane. These two effects may finally induce birth of microvesicles which budded off from protuberant parts on a mother vesicle [28]. Since the transition of the biconcave shape of red blood cells to the echinocyte one occurring *in vivo* and *in vitro* under various different situations is highly complicated, the present theoretical explanation of the transition may be too naive

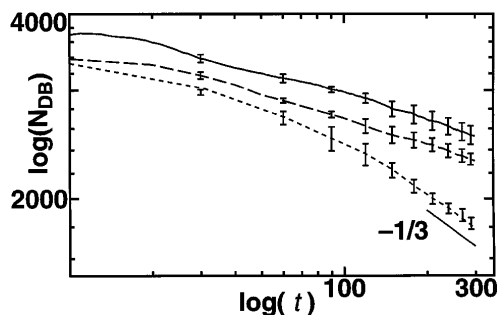


FIG. 3. Same as Fig. 2 but for three off-critical quenches $\langle\phi\rangle = 0.3$, (1) $\Lambda = 0.8$ (solid line), (2) $\Lambda = 0.5$ (dashed line), and (3) $L_r = 0$ and $\Lambda = 0$ (dotted line).

to explain the real situations. In fact, the membrane of the red blood cell is composed of many components (e.g., intramembrane proteins, multicomponent lipids, a spectrin network in the cytoplasmic side, and so on). Moreover, pH of a solvent inside the cell influences the shape of the vesicle. These complicated elements of real biomembranes are not taken into account in our model. It seems, however, that many experimental evidences support that the local coupling between the composition and the curvature of the membrane plays a crucial role in the formation of the echinocytosis [29]. Experiments on dynamics of two-component fluid membranes on which a phase separation takes place are very informative to check the validity and limitation of the present dynamical model and to construct a more realistic model.

The author greatly acknowledges Professor Toshihiro Kawakatsu, Dr. Kazuhiro Fuchizaki, and Professor Akira Onuki for helpful discussions. This work is supported by the Grant-in-Aid for Encouragement of Young Scientists, from Ministry of Education, Science and Culture, Japan. The computation in this work has been done using the facilities of the Supercomputer Center, Institute for Solid State Physics, University of Tokyo.

*Electronic address: taniguch@ton.scpphys.kyoto-u.ac.jp

- [1] W. Helfrich, *Z. Naturforsch* **28C**, 693 (1973).
- [2] *Statistical Mechanics of Membranes and Surfaces*, edited by D. R. Nelson *et al.* (World Scientific, Singapore, 1989).
- [3] B. Deuticke, *Biochim. Biophys. Acta* **163**, 494 (1968).
- [4] M. P. Sheetz and S. J. Singer, *Proc. Natl. Acad. Sci. U.S.A.* **74**, 4475 (1974); M. P. Sheetz, R. G. Painter, and S. J. Singer, *J. Cell Biol.* **70**, 193 (1976).
- [5] S. Leibler, *J. Phys. (France)* **47**, 507 (1986); S. Leibler and D. Andelman, *ibid.* **48**, 2013 (1987).
- [6] R. Morikawa and Y. Saito, *J. Phys. Soc. Jpn.* **64**, 3562 (1995).
- [7] D. Andelman, T. Kawakatsu, and K. Kawasaki, *Europhys. Lett.* **19**, 57 (1992).
- [8] T. Taniguchi, K. Kawasaki, D. Andelman, and T. Kawakatsu, *Cond. Matt. Materials Comm.* **1**, 75 (1993).
- [9] T. Kawakatsu, D. Andelman, K. Kawasaki, and T. Taniguchi, *J. Phys. II (France)* **3**, 971 (1993).
- [10] T. Taniguchi, K. Kawasaki, D. Andelman, and T. Kawakatsu, *J. Phys. II (France)* **4**, 1333 (1994).
- [11] U. Seifert, *Phys. Rev. Lett.* **70**, 1335 (1993).
- [12] R. Lipowsky, *J. Phys. II (France)* **2**, 1825 (1992); F. Jülicher and R. Lipowsky, *Phys. Rev. Lett.* **70**, 2964 (1993).
- [13] C. Gebhardt, H. Gruler, and E. Sackmann, *Z. Naturforsch. C* **32**, 581 (1977). A lateral phase separation of fluid-fluid phases has been observed by S.H. Wu and H.M. McConnell, *Biochem.* **14**, 847 (1975).
- [14] A. Onuki, *J. Phys. Soc. Jpn.* **62**, 385 (1993).
- [15] S. Mori and M. Wadati, *J. Phys. Soc. Jpn.* **62**, 3557 (1993).
- [16] G. Foltin, *Phys. Rev. E* **49**, 5243 (1994).
- [17] W. Cai and T. C. Lubensky, *Phys. Rev. Lett.* **73**, 1186 (1994).
- [18] In experiments of the transformation of red blood cells to the echinocyte [3,4], externally added amphiphiles are preferentially intercalated into one of the two sides of a bilayer depending on the kind of the head part of the amphiphile. The simple situation used here can be regarded as an idealization of such experiments.
- [19] We assume that the amphiphiles within the membrane do not diffuse into the surrounding solution due to their hydrophobic tails and do not flip between the inner layer and the outer layer of the bilayer. The latter assumption is justified by an observation that the flip flop is extremely slower than the lateral diffusion. See R. D. Kornberg and H. M. McConnell, *Biochem.* **10**, 1111 (1971).
- [20] J. T. Jenkins, *J. Math. Biol.* **4**, 149 (1976).
- [21] Detailed derivations of Eqs. (4)–(7) and the method of the simulation will be given elsewhere.
- [22] Ou-Yang Zhong-can and W. Helfrich, *Phys. Rev. Lett.* **59**, 2486 (1987); *Phys. Rev. A* **39**, 5280 (1989).
- [23] In deriving Eqs. (5) and (6), we used the relations $\delta \mathbf{r}(u)/\delta \mathbf{r}(u') = \delta \phi(u)/\delta \phi(u') = \delta(u^1 - u'^1)\delta \times (u^2 - u'^2)/\sqrt{g}$.
- [24] R. Edberg, D. J. Evans, and G. P. Morris, *J. Chem. Phys.* **84**, 6933 (1986).
- [25] A lattice point is counted in N_{NB} if at least one of the ϕ 's in its six (or five) nearest neighbor lattice points has the opposite sign to that of ϕ at that lattice point.
- [26] The coarsening dynamics for $\langle \phi \rangle = -0.3$ is the almost same feature as that for $\langle \phi \rangle = 0.3$ in Fig. 3.
- [27] The coarsening law $t^{-1/3}$ of the total length of domain boundaries on the rigid sphere holds until $t \approx 3000$, where the domain size reaches the system size.
- [28] D. Allan, M. M. Billah, J. B. Finean, and R. H. Michell, *Nature (London)* **261**, 58 (1976).
- [29] See discussions by S. Leibler in Ref. [5] and by V. S. Markin, *Biophys. J.* **36**, 1 (1981), and references therein.